

## SUPPLEMENTARY MATERIAL

### Water softening using graphene oxide/biopolymer hybrid nanomaterials

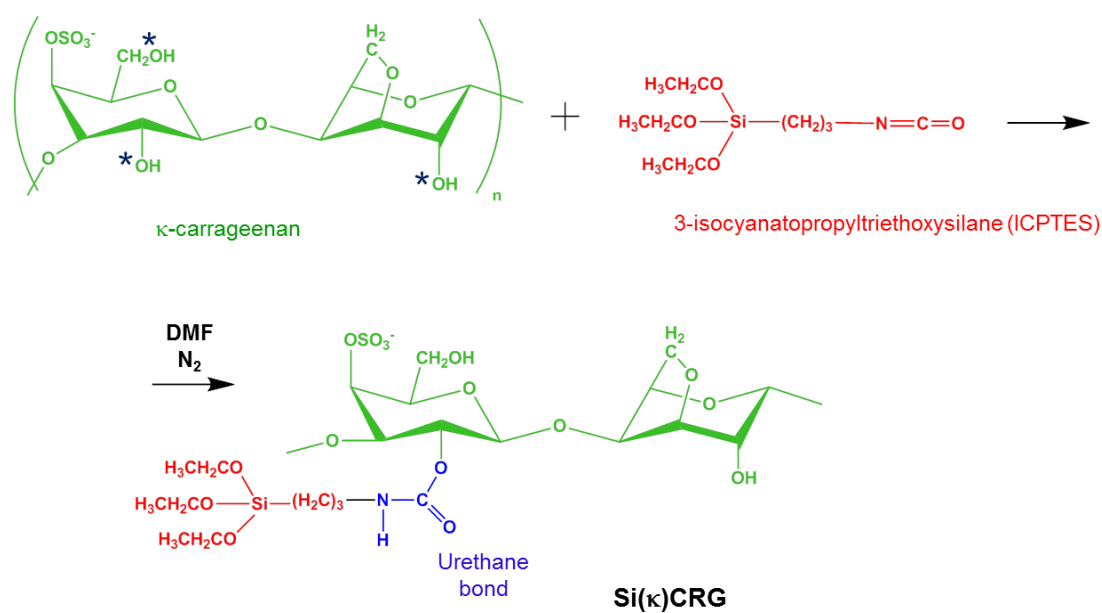
Luciana S. Rocha<sup>1</sup>, João Nogueira<sup>1</sup>, Ana Luísa Daniel-da-Silva<sup>1\*</sup>, Paula Marques<sup>2</sup>, Sara Fateixa<sup>1</sup>, Eduarda Pereira<sup>3</sup> & Tito Trindade<sup>1</sup>

<sup>1</sup> CICECO, Department of Chemistry, University of Aveiro, 3810-193 Aveiro, Portugal.

<sup>2</sup> TEMA-NRD, Mechanical Engineering Department, University of Aveiro, 3810-193 Aveiro, Portugal

<sup>3</sup> LAQV-REQUIMTE & CESAM, Department of Chemistry, University of Aveiro, 3810-193 Aveiro, Portugal.

#### S1. Synthesis of biopolymer–GO hybrid



**Scheme S1.** Scheme of the synthesis of Si( $\kappa$ )CRG, by reaction of the hydroxyl groups of  $\kappa$ -carrageenan with isocyanate groups of ICPTES (\* target reactive sites for isocyanate groups).

## S2. Sorption and equilibrium models

### i) Kinetic models

The process of the formation of a molecular layer of the sorbate on the surface of the sorbent involves several steps with distinct rates: bulk diffusion, film diffusion, intra-particle diffusion, and finally physical or chemical sorption onto the surface. Two main classes can be defined for the sorption kinetic models: reaction and diffusion based models. In the reaction-based models the interaction between the sorbent and the sorbate, i.e. the last step, is considered to be the slowest process and that the sorbate uptake on the material is of chemical nature [1]. In the present study, the experimental kinetic data was adjusted to pseudo-first order (Eq. S1), pseudo-second order (Eq. S2) and Elovich (Eq. S3) reaction-based models, the ones described by the following equations [2][3]:

$$q_t = q_e (1 - e^{-k_1 t}) \quad (\text{S1})$$

$$q_t = \frac{q_e^2 k_2 t}{1 + q_e k_2 t} \quad (\text{S2})$$

$$q_t = \frac{1}{\beta} \ln(1 + \alpha \beta t) \quad (\text{S3})$$

in which  $k_1$  ( $\text{h}^{-1}$ ) is the pseudo-first order (P1<sup>st</sup>O) rate constant,  $k_2$  ( $\text{g mg}^{-1} \text{h}^{-1}$ ) the pseudo-second order (P2<sup>nd</sup>O) rate constant,  $\alpha$  ( $\text{mg g}^{-1} \text{h}^{-1}$ ) the initial sorption rate and  $\beta$  ( $\text{g mg}^{-1}$ ) the desorption constant.

The diffusion-based models presuppose that one or more of the diffusion steps are the rate-controlling factor. This frequently happens when the surface of the sorbent is relatively inert and solely physical sites are available for bond formation [2]. Two diffusional models are currently used: Webber's intraparticle diffusion (Eq. S4) and Boyd's film diffusion (Eqs. S5 and S6) [2][4][5]:

$$q_t = k_{id} t^{1/2} \quad (\text{S4})$$

$$Bt = -0.4977 - \ln(1 - F), \text{ for } F \text{ values} > 0.85, \quad (\text{S5})$$

$$Bt = \left( \sqrt{\pi} - \sqrt{\pi - \frac{\pi^2 F}{3}} \right)^2, \text{ for } F \text{ values} < 0.85 \quad (\text{S6})$$

where  $k_{id}$  is the internal diffusion rate constant ( $\text{mg g}^{-1} \text{min}^{-1/2}$ ),  $F(t)$  is the fractional attainment of equilibrium at times  $t$  and  $Bt$  is a function of  $F$ . For  $F > 0.85$ , Equation S5 was used in the determination of  $Bt$  and for  $F < 0.85$ , Equation S6 was applied.

## ii) Equilibrium models

The information regarding the affinity or capacity of the sorbent material in a particular sorption process can be afforded through the construction of the isotherms [6][2]. In the present work, Langmuir (Eq. S7), and Freundlich (Eq. S8) equations were used to model the equilibrium data. The Langmuir model assumes the formation of a monolayer coverage and the existence of a finite number of binding sites, homogeneously distributed along the sorbent surface. As for the Freundlich model, it assumes adsorption on heterogeneous surfaces with sorption sites of varying energy and that adsorption can occur based on multiple layers. These models are defined as followed:

$$q_e = \frac{q_{mL} a_L C_e}{1 + a_L C_e} \quad (S7)$$

$$q_e = K_F C_e^{1/n'} \quad (S8)$$

where  $a_L$  ( $L \text{ mg}^{-1}$ ) is the Langmuir sorption equilibrium constant, related to the bonding energy of sorption, and  $q_{mL}$  ( $\text{mg g}^{-1}$ ) is the Langmuir sorption capacity corresponding to complete monolayer coverage;  $K_F$  ( $\text{mg}^{1-1/n'} \text{ L}^{1/n'} \text{ g}^{-1}$ ) is the Freundlich equilibrium constant and  $n'$  is the sorption intensity constant (usually  $1/n'$  varies between 0.1 and 1, indicating favorable sorption) [7][8][9].

### *S3. Error analysis of the data*

The Akaike's Information Criterion (*AIC*) and the evidence ratio were calculated using Eq. (9) and (10), respectively:

$$AIC = N \ln \left( \frac{SSE}{N} \right) + 2N_p + \frac{2N_p(N_p+1)}{N-N_p-1} \quad (9)$$

$$Evidence\ ratio = \frac{1}{e^{-0.5\Delta}} \quad (10)$$

where  $N$  is the number of experimental data points,  $N_p$  the number of parameters in the model,  $SSE$  is the sum of squared deviations and  $\Delta$  is the absolute value of the difference in *AIC* between the two models.

#### S4. Zeta potential measurements

The surface charge of GO and GO-Si( $\kappa$ )CRG nanomaterials was assessed by zeta potential measurements at variable pH, and the data obtained are depicted in Figure S1.

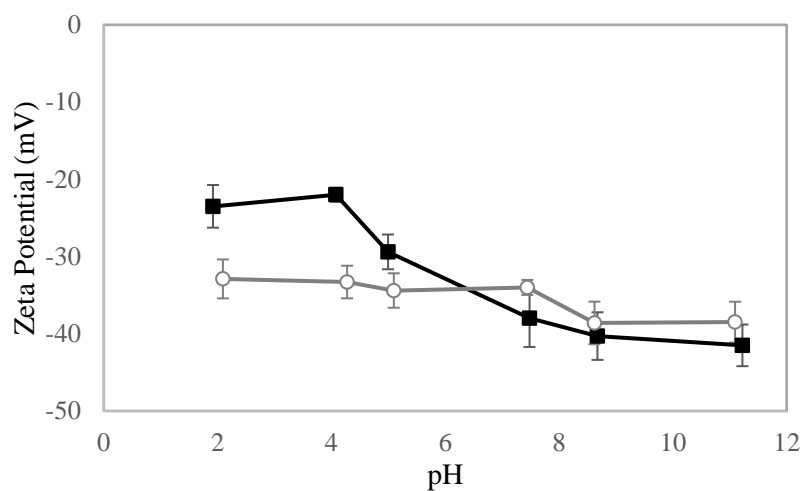


**Figure S1.** Zeta potential measurements for GO (■) and GO-Si( $\kappa$ )CRG (○).

S5. Boyd's diffusion model

Figure S2 presents the Boyd's plot ( $Bt$  vs  $t$ ) in the beginning of the sorption ( $t \leq 20$  minutes) of  $\text{Ca}^{2+}$  onto GO-Si( $\kappa$ )CRG, using different experimental conditions.

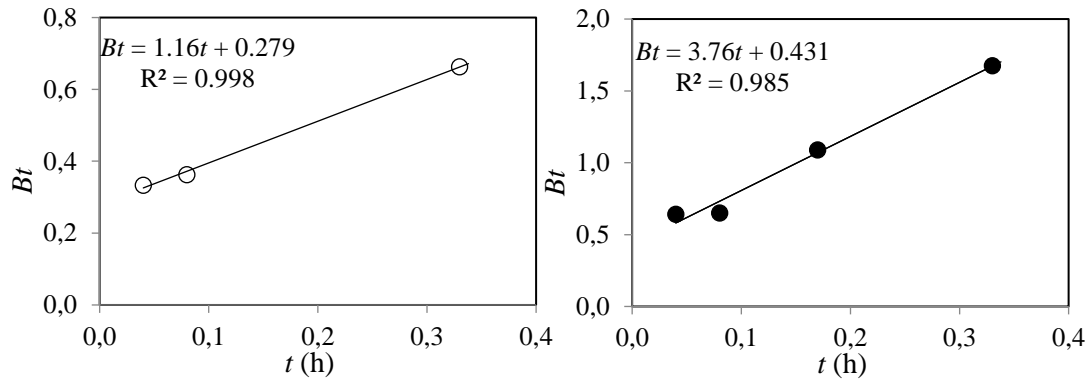


**Figure S2.** Boyd plots for the initial period of sorption ( $t \leq 0.33$  h) of  $\text{Ca}^{2+}$  onto GO-Si( $\kappa$ )CRG for the following experimental conditions:  $C_{\text{Ca},0} = 30$  mg/L e  $m/V = 1.0$  g/L ( $\circ$ ) e  $C_{\text{Ca},0} = 120$  mg/L e  $m/V = 5.0$  g/L ( $\bullet$ ).

### *S6. Standard free energy change ( $\Delta G^\circ$ )*

The standard free energy change ( $\Delta G^\circ$ ) was calculated using the Eq. (11) [10]:

$$\Delta G^\circ = -RT \ln K \quad (11)$$

where  $K$  is the equilibrium constant for the sorption interaction,  $T$  is the temperature in Kelvin and  $R$  is the gas constant (8.314 J/(mol.K)). The value of  $K$  was calculated following the method suggested by Lima et al. [11]. Accordingly, the Langmuir equilibrium constant was converted in the dimensionless form by multiplying by the molecular weight of the adsorbate ( $C_a$ ). The resulting dimensionless value of  $K$  was employed in the equation 11. The value of  $\Delta G^\circ$  obtained for the adsorption of  $\text{Ca}^{2+}$  on GO-Si( $\kappa$ )CRG sorbent at  $21 \pm 2^\circ\text{C}$  was  $-16.67 \text{ kJ mol}^{-1}$ .

### S7. ATR-FTIR spectra

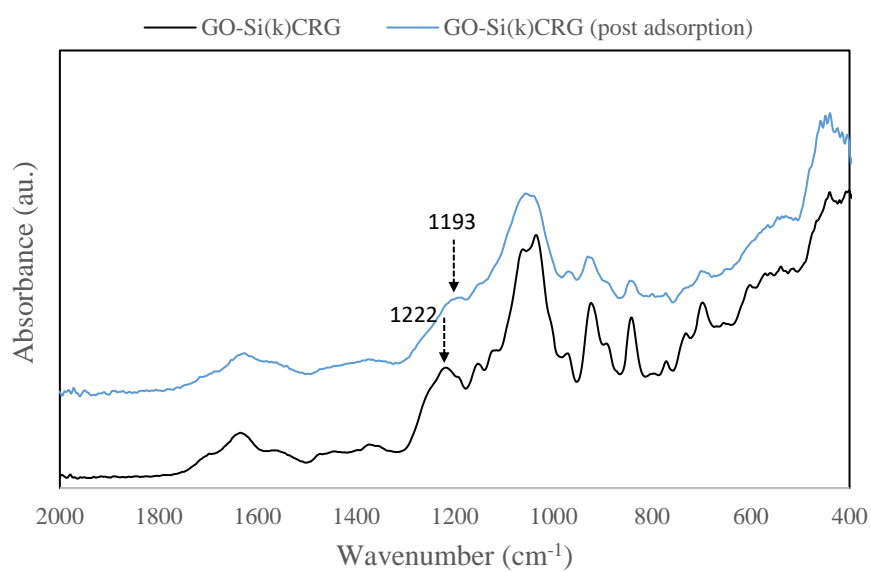


**Figure S3.** ATR-FTIR spectra for GO-Si( $\kappa$ )CRG prior (—) and after (—) the adsorption experiments with Ca<sup>2+</sup>.



## REFERENCES

- [1] G. Crini, E. Lichtfouse, L. Wilson, N. Morin-crini, G. Crini, E. Lichtfouse, L. Wilson, N.M. Adsorption-oriented, G. Crini, E. Lichtfouse, L.D. Wilson, N. Morin-crini, Adsorption-oriented processes using conventional and non-conventional adsorbents for wastewater treatment. *Green Adsorbents for Pollutant Removal*, Springer Nature, 2018. [https://doi.org/10.1007/978-3-319-92111-2\\_2](https://doi.org/10.1007/978-3-319-92111-2_2).
- [2] Y.S. Ho, J.C.Y. Ng, G. McKay, Kinetics of Pollutant Sorption by Biosorbents: Review, *Sep. Purif. Methods*. 29 (2000) 189–232. <https://doi.org/10.1002/chin.200147289>.
- [3] Y.S. Ho, Review of second-order models for adsorption systems, *J. Hazard. Mater.* 136 (2006) 681–689. <https://doi.org/10.1016/j.jhazmat.2005.12.043>.
- [4] G.F. Malash, M.I. El-Khaiary, Piecewise linear regression: A statistical method for the analysis of experimental adsorption data by the intraparticle-diffusion models, *Chem. Eng. J.* 163 (2010) 256–263. <https://doi.org/10.1016/j.cej.2010.07.059>.
- [5] M.I. El-Khaiary, G.F. Malash, Common data analysis errors in batch adsorption studies, *Hydrometallurgy*. 105 (2011) 314–320. <https://doi.org/10.1016/j.hydromet.2010.11.005>.
- [6] D. Park, Y.S. Yun, J.M. Park, The past, present, and future trends of biosorption, *Biotechnol. Bioprocess Eng.* 15 (2010) 86–102. <https://doi.org/10.1007/s12257-009-0199-4>.
- [7] J. Wang, C. Chen, Biosorbents for heavy metals removal and their future, *Biotechnol. Adv.* 27 (2009) 195–226. <https://doi.org/10.1016/j.biotechadv.2008.11.002>.
- [8] Y.S. Ho, J.F. Porter, G. McKay, Divalent Metal Ions Onto Peat : Copper , Nickel and Lead Single Component Systems, *Water. Air. Soil Pollut.* 141 (2002) 1–33. <https://doi.org/10.1023/A:1021304828010>.
- [9] E.I. El-Shafey, Removal of Zn ( II ) and Hg ( II ) from aqueous solution on a carbonaceous sorbent chemically prepared from rice husk, *J. Hazard. Mater.* 175 (2010) 319–327. <https://doi.org/10.1016/j.jhazmat.2009.10.006>.
- [10] S.G. Nanaki, G.Z. Kyzas, A. Tzereme, M. Papageorgiou, M. Kostoglou, D.N. Bikiaris, D.A. Lambropoulou, Synthesis and characterization of modified carrageenan microparticles for the removal of pharmaceuticals from aqueous solutions, *Colloids Surfaces B Biointerfaces*. 127 (2015) 256–265. <https://doi.org/10.1016/j.colsurfb.2015.01.053>.

- [11] E.C. Lima, A. Hosseini-Bandegharai, J.C. Moreno-Piraján, I. Anastopoulos, A critical review of the estimation of the thermodynamic parameters on adsorption equilibria. Wrong use of equilibrium constant in the Van't Hoof equation for calculation of thermodynamic parameters of adsorption, *J. Mol. Liq.* 273 (2019) 425–434. <https://doi.org/10.1016/j.molliq.2018.10.048>.